CHEMICAL VAPOR DEPOSITED PERMEATION BARRIERS IN TEFLON EXPULSION BLADDERS

D. FRANK BAZZARRE* and JOHN PETRIELLO**
*Commonwealth Scientific Corporation
**Dilectrix Corporation

May 68

I. INTRODUCTION

This paper will primarily deal with the reduction of N_2O_4 permeation in Teflon expulsion bladders, through the utilization of chemical vapor deposited aluminum coatings in thicknesses from 0.0001 to 0.001 inches. The primary purpose of this work was to develop a high reliability process to incorporate continuous, conforming, aluminum permeation barriers within Teflon wall constructions.

As a general background, permeation rates as applied to Teflon expulsion bladders are related to the specific bladder film construction. It is fairly common knowledge that for a given thickness of film the homopolymer TFE exhibits a higher permeation rate than its copolymer FEP by a factor approximating 7. For reasons involving this characteristic as well as other physical parameters, the preponderance of Teflon bladders in past and current use have employed a laminate of TFE and FEP. The relative permeation rates through typical 10 mil wall structures with N_2O_4 as the permeant would be measured as follows:

TFE	-	5.0 mg/sq.in/hr
TFE/FEP Laminate	-	2.7 mg/sq.in/hr

Incorporation of a pre-treated rolled thin aluminum foil within the laminate construction have been employed as highly effective permeation barriers against both N_2O_4 propellant and helium expellant gas. Such a bladder structure was proven to be successful in the reaction control systems of the Lunar Orbiter vehicles. In general, aluminum and gold rolled metal foils have been employed as the permeation barriers in both polymeric and elastomeric systems. Two problems arise in using metal foils, the first and probably more serious is a marked rise in the specific modulus of bladder construction due to extensive cold working of the foil in mill rolling to reduce its thickness to the range of 0.0002 to 0.002 inches and the nonavailability of effective heat treatments to anneal after rolling. Additionally, it is of course necessary that the coated flat sheet of metal foil be arranged to conform to the compound surface curvatures of spherical as well as hemispherical mandrel forms. Normally gore strips or segments are laid up on a preform and

DISCLAIMER NOTICE

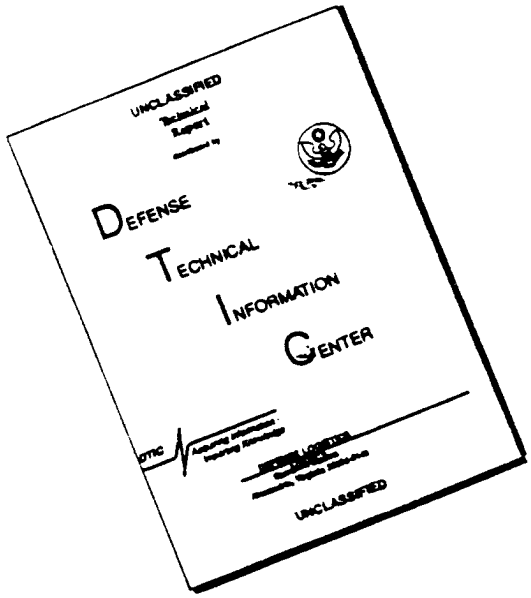

THIS DOCUMENT IS BEST QUALITY AVAILABLE. THE COPY FURNISHED TO DTIC CONTAINED A SIGNIFICANT NUMBER OF PAGES WHICH DO NOT REPRODUCE LEGIBLY.

then transposed to the mandrel. This segmentation obviously results in overlap seams, and at certain critical joining areas, in multiple overlaps of metallic foil. Further, the rolled metal foils exhibit an inherently high specific modulus which results in a Teflon/foil construction of limited flex life with respect to pinholding of the foil. With these two problems associated with the otherwise exceptional performance of metallic permeation barriers in Teflon, we set out on an approach to form one piece, seamless permeation barriers. Aluminum was selected as the barrier material on the basis of its past performance as a permeation barrier. It was ascertained that deposition would be the only process by which a continuous and uniform barrier could be applied to Teflon. Three candidate systems were investigated, these were vacuum evaporation, chemical vapor deposition and electrodeposition. Each was considered carefully; vacuum deposition was discounted through previous experience by Dilectrix due to inherent limitations in depositing films substantially thicker than 20-60 millionths inches thick, and the fact that vacuum deposition is the condensation of metallic spheres on the coated substrate, and spheres do not produce a tight stacking latice therefore generating leak paths for propellants and gases. Electrodeposition was discounted for several reasons; prior to electrodepositing a coating the substrate must be made electrically conductive by vacuum evaporation, chemical reduction or metallic painting, none of which prove satisfactory for producing pin hole free coatings. The next significant problem associated with electrodeposition of aluminum is the fact that the process is extremely hard to control, so as to produce stress free, low modulus coatings. Therefore, with each of these considerations for vacuum evaporation and electrodeposition, chemical vapor deposition was investigated.

Chemical vapor deposited aluminum was found to be readily applied to Teflon in a very adherent manner and in a "pin hole" free condition. The process appeared to be readily carried out in a reasonable approach consistant with present production practices with no distinct problems. It was therefore decided to further investigate C.V.D. aluminum as a possible permeation barrier.

2. INCORPORATION OF C.V.D. ALUMINUM PERMEATION BARRIER

Several areas for bladder fabrication were well established from previous work. These were the formation of the Teflon bladder and the formation of the aluminum coating, the areas for further investigation were in preparing a composite of Teflon and aluminum. Areas studied were:

(1) Bonding of the C.V.D. aluminum to Teflon insitu.

(2) Develop lowest possible modulus C.V.D. aluminum

(3) Develop crystal structure in C.V.D. aluminum with the highest mean free resistance to permeation.

(4) Develop mechanical properties of composite to perform satisfactorily as bladder material.

Each of these four areas were thoroughly investigated.

2.1 Bonding.

Three conditioners were studied to promote satisfactory bonding of C.V.D. aluminum to Teflon films. These were:

(1) Chemical cleaning

(2) Vapor Honing

(3) Sodium Etching

Chemical cleaning was accomplished after the Teflon films were sintered at 680° by thoroughly soaking in acetone and then drying at 570°f in a nitrogen atmosphere. Vapor honing was carried out on sintered films with -325 mesh Al_2O_3 in a water slurry under 40 psi air pressure. The sodium etching was carried out using one of the commercially available etchants in an inert atmosphere. Each of the surface preparation techniques investigated produce satisfactory bonding for bladder performance although the chemical cleaning produces superior bonding in long term N_2O_4 soaking.

2.2 Selection of Aluminum

Four organometallic compounds were investigated as the aluminum source for the C.V.D. aluminum films, these were:

(1) Triisobulylabuminum (TIBA)

(2) Diisobulylaluminum hydride (DiBAl)

(3) Tri normal propylaluminum (TNP)

(4) Diethylaluminum hydride (DEAH)

It was found that the modulus of the resulting aluminum barrier was directly related to its chemical purity (i.e., high purity - low modulus). The lowest modulus films

were produced from TIBAI - and these exhibited a modulus in the order of 8.5 X 10^6 psi with elongation of 67%. The purity of this material is less than 100 ppm total foreign matter. The modulus ranged to 14 X 10^6 psi with diethylaluminum hydride with total impurities reaching a level of 2%. The major impurity in this coating was carbon.

2.3 Selection of Teflon Bladder Construction

Two bladder constructions were investigated, these were TFE and co-dispersions of TFE and FEP. Initial coating efforts, however, indicated several problems attributable to the co-dispersion. Since the magnitude of the program did not permit complete parallel efforts, concentration was placed on the TFE as a base material.

The process of construction consisted of coating a 0.004 inch film of TFE with 0.0001 - 0.001 inches of C. V. D. aluminum and applying an overlay of TFE of 0.004 inches (see FigA). This process worked very effectively to produce a wall construction of approximately 0.008 inches.

2.4 Aluminum Deposition Temperature

Several deposition temperatures were investigated with each of the aluminum organometallic compounds, these ranged from 240-290°C. The lower temperatures produced the most desirable deposits, from a purity standpoint, the higher temperatures tended to produce slight reactions with the TFE during deposition. With this data 240°C was selected as the optimum deposition temperatures.

2.5 Controlled Crystalline Structure

This entire investigation was predominantly concerned with producing low permeation materials. It was felt that with the C. V. D. process, the crystalline structure is the single most important factor influencing permeation therefore extensive studies were conducted in this area. The first decision point reached was how to examine the crystalline structure of thin film (less than 0.0003 inches) aluminum deposites. Several approaches were investigated:

(1) Optical microscopy
(2) Xray Diffraction
(3) Xray Fluorescence
(4) Electron Microscope

Of these four methods only the electron microscope was satisfactory. Carbon replication was successfully employed and indicated detailed crystal structure. The electron scanning microscope was also quite successfully employed. Five samples in this sequence were examined with the scanning electron microscope. By this technique adequate resolution can be achieved so that crystal structure of the Figures 1 and 2 show a comparison between optical and scanning electron microscopy. It is clear that the use of the scanning electron microscope is more advantageous not only because of its superior resolving power but also its depth of field.

Figures 1, 3 and 4 are scanning electron photomicrographs showing a topographic view of sample number S/N 091-432 at three magnifications. It is apparent that the chemically vapor deposited aluminum film is composed of interwoven lamellar microcrystallites. The compact stacking arrangement is shown clearly in Figure 4. The crystallites, which appear generally to be oriented parallel to the substrate surface, exhibit a pseudo-hexagonal habit. Plating parameters for this sample are given in Table 1.

TABLE I

PLATING PARAMETERS FOR SAMPLES EXAMINED BY SCANNING ELECTRON MICROSCOPY

Sample No.	Al Source	Suppressant	Depn. Temp -°C	Crystal Structure
402	TIBAL	Isobutylene	255	Columnar
426	TNPAL	None	250	Agglomerate
415	TIBAL	Ethylene	255	Lamellar
432	TNPAL	Ethylene	290	Lamellar

Figure 5 is a scanning electron photomicrograph of sample number S/N 091-415. Again the interwoven, lamellar structure is seen; although the crystallite stacking is not so compact as in sample number S/N 091-432, Figure 3. These two samples, which represent a significant variation in plating compound and deposition temperature, Table I,

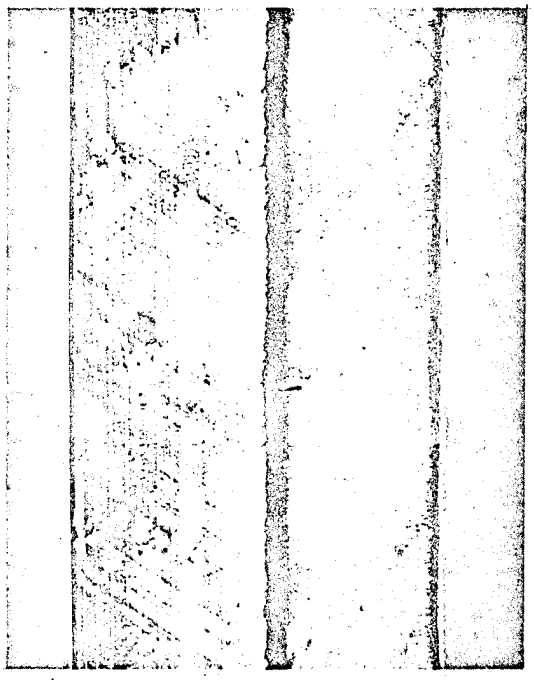

FIGURE A
TFE - ALUMINUM - TFE
BLADDER CONSTRUCTION.

indicate that crystal structure is more dependent on suppressant agent than on other parameters. Both samples were prepared with ethylene as the suppressant. Figure 6 and 7 are scanning electron photomicrographs showing two different views of sample number S/N 091-434. A topographical picture of a replication of the chemically vapor deposited aluminum film is represented. An interwoven platelet structure is clearly indicated. As shown in Table I, this sample was prepared with propylene as the suppressant. Ethylene and propylene might be expected to have similar effects on crystal growth because of their related chemical structures. The TNPAL - propylene system was proposed as an alternate route, on the basis of physical properties. A scanning electron photomicrograph of sample S/N 091-426 is shown in Figure 8. Individual aluminum particles, seen as small agglomerates, exhibit an open structure in contrast to the interwoven platelets previously described. The primary difference between plating parameters for samples S/N 091-426 and S/N 091-434 was the suppressing agent, as shown in Table I. Again the significance of this factor on crystal structure becomes apparent.

Figure 9 is a scanning electron photomicrograph of a replicated surface of sample number S/N 091-402. The regular structure indicates a columnar type of growth with crystallites oriented perpendicular to the substrate. From Table I it may be seen that the condition for samples S/N 091-402 and S/N 091-415 were identical except for the suppressant agent.

The lamellar structure is suspected to be less permeable than the columnar or agglomerate structures because it offers a much greater mean free path. Permeation would be expected to follow crystallite grain boundaries.

Deformation was performed on several of the samples by applying a tensile stress to strips of the aluminum coated teflon 0.5 cm x 5.0 cm. With initial stress application homogeneous deformation occurred. Figure 10 is a scanning electron photomicrograph of sample number S/N 091-432 after light deformation. Comparison with Figure 1 indicates little difference in microstructure between the undeformed and lightly deformed samples. However, cracks in the aluminum film may be seen in Figure 5, designated UV and intersecting cracks KL and MN. Such cracks were not observed in the undeformed sample and are apparently the result of accommodation of the applied stresses. Light deformation of this sample also appears to cause displacement of individual crystallites. It may be seen in Figure 11 that the interwoven stacking pattern, characteristic of the undeformed sample, Figure 3, has been modified to a more open structure by a gliding of individual crystallites over each other.

Application of additional stress to sample number S/N091-432 produced a region of major deformation. Figure 12 shows the aluminum film to be highly disrupted. In Figure 13 the crystallites appear to have regained this interwoven structure (compare with Figure 4) after the formation of rupture line PQ. It is possible that as rupture of the aluminum film occurs the crystallites return to a low energy configuration. In contrast to the lamellar films, the agglomerate structure of sample number S/N 091-426 obviously lacks the ability for glide of individual crystals to occur. Figures 14 and 15 show the aluminum film to be cracked before any deformation stress is applied.

3. RESULTS

The results obtained to date have been very encouraging. The permeation rate to N_2O_4 has been dropped from the normal range of 5-6mg/in^2/hr in a 10 mil TFE construction to 0.1 mg/in^2/hr with 0.0003 inch C. V. D. aluminum films in the same construction. The modulus of the finished constructions vary from 100-200 x 10^3psi which compares with an all TFE construction of 60-70 x 10^3psi. Finished constructions have been elongated 50-80% without failure of the aluminum barrier. Roll and crease tests show promising data. The step forward to produce the lamellar interwoven crystal structure appears not only to have decreased the permeation rate but also to have significantly lowered the modulus of the finished wall construction. The most significant development of this entire investigation has been the establishment of a method to produce uniform metallic permeation barriers for use with expulsion mechanisms, which have no seams, welds,

overlaps, or discontinuities and maintains the basic physical properties associated with Teflon constructions.

The production of expulsion bladders employing C. V. D. aluminum permeation barriers will be readily undertaken in mass production utilizing predictable quality control techniques to insure the highest quality mechanisms.

Acknowledgement:
The Authors wish to express their gratitude to the Jet Propulsion Laboratory for permission to publish this paper on work conducted under contract with this facility.

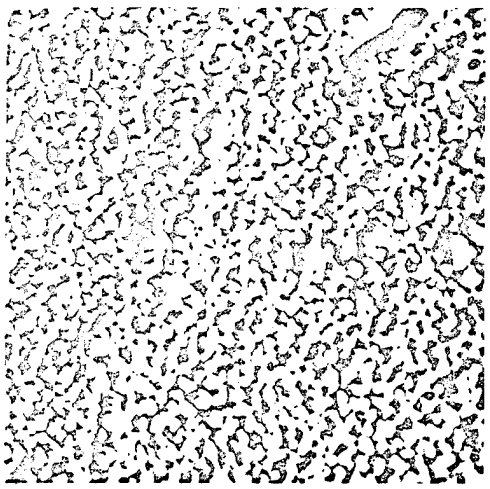

FIGURE 1

SCANNING ELECTRON PHOTOMICROGRAPH
OF SAMPLE NO. S/N 091-432 AT 300X

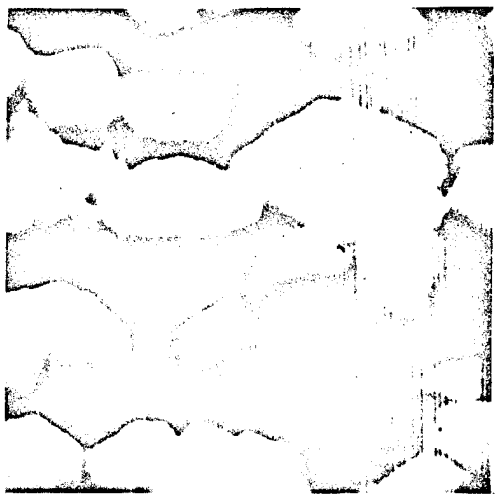

FIGURE 3

SCANNING ELECTRON PHOTOMICROGRAPH
OF SAMPLE NO. S/N 091-432 AT 5,000X

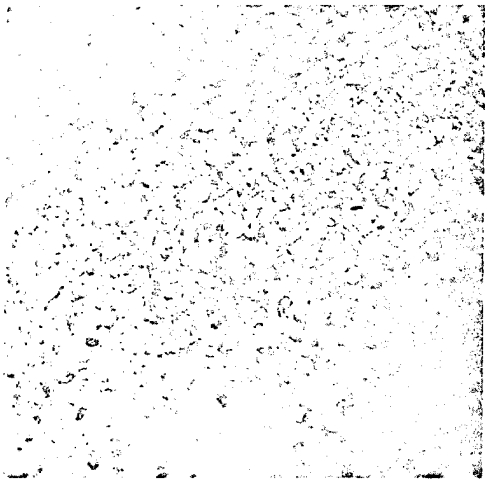

FIGURE 2
OPTICAL PHOTOMICROGRAPH
OF SAMPLE NO. S/N 091-432 AT 560X

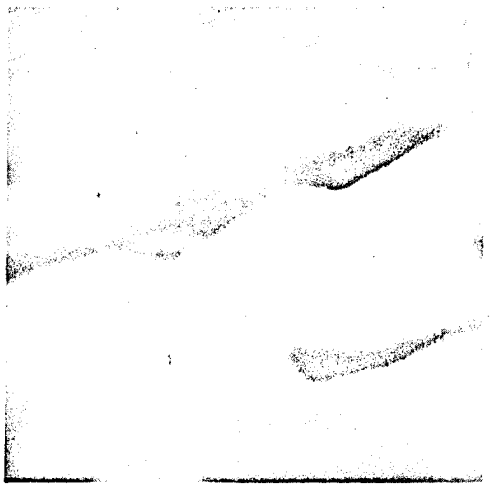

FIGURE 4
SCANNING ELECTRON PHOTOMICROGRAPH
OF SAMPLE NO. S/N 091-432 AT 10,000X

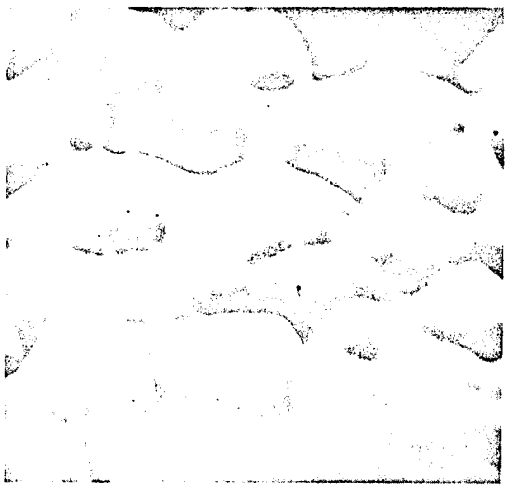

FIGURE 5
SCANNING ELECTRON PHOTOMICROGRAPH
OF SAMPLE NO. S/N 091-415 AT 5,000X

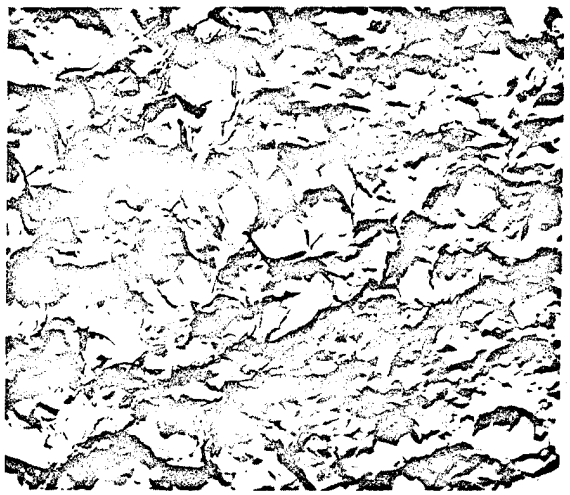

FIGURE 6
SCANNING ELECTRON PHOTOMICROGRAPH
OF A REPLICATED SURFACE
OF SAMPLE NO. S/N 091-434, VIEW A,
AT 5,000X

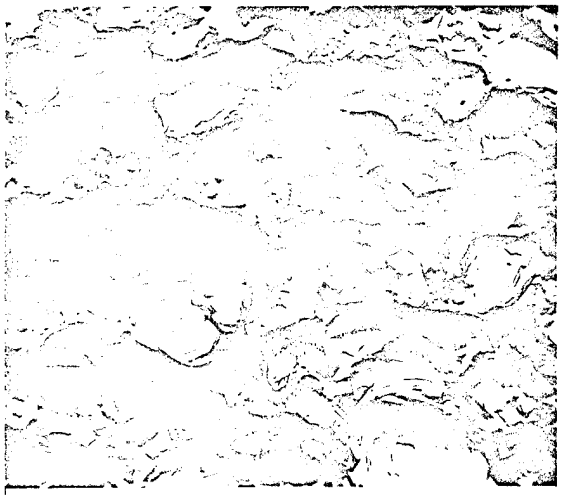

FIGURE 7

SCANNING ELECTRON PHOTOMICROGRAPH
OF A REPLICATED SURFACE
OF SAMPLE NO. S/N 091-434, View B
AT 5,000X

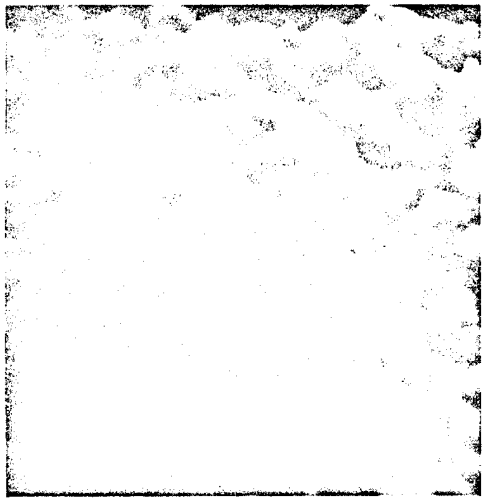

FIGURE 8

SCANNING ELECTRON PHOTOMICROGRAPH
OF SAMPLE NO. S/N 091-426 AT 1,000X

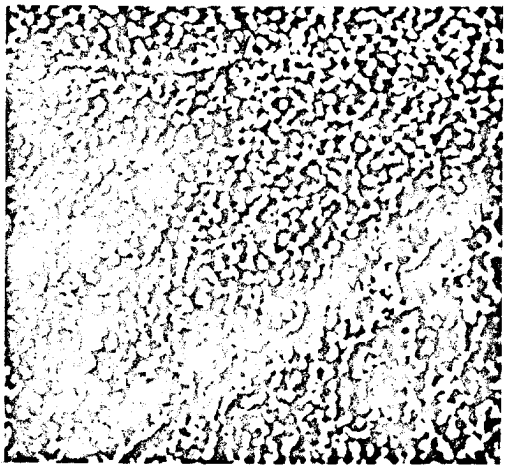

FIGURE 10
SCANNING ELECTRON PHOTOMICROGRAPH
OF SAMPLE NO. S/N 091-432 AT 300X
AFTER LIGHT DEFORMATION

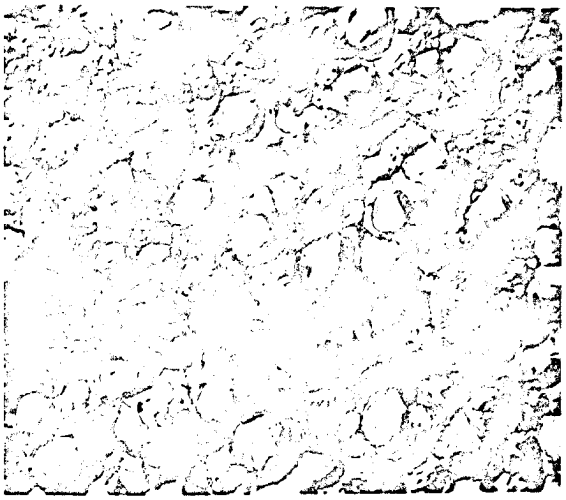

FIGURE 9
SCANNING ELECTRON PHOTOMICROGRAPH
OF A REPLICATED SURFACE
OF SAMPLE NO. S/N 091-402 AT
5,000X

FIGURE 11
SCANNING ELECTRON PHOTOMICROGRAPH
OF SAMPLE NO. S/N 091-432 AT 5,000X
AFTER LIGHT DEFORMATION

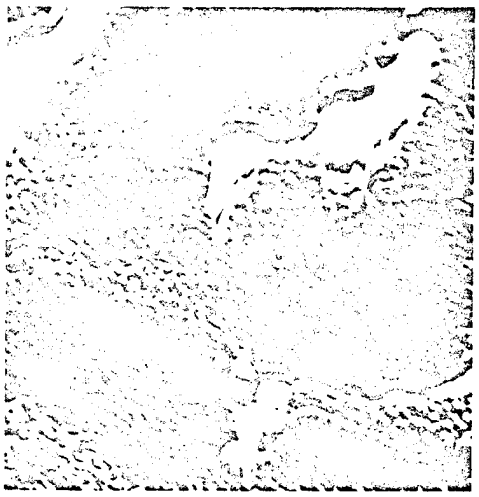

FIGURE 12
SCANNING ELECTRON PHOTOMICROGRAPH
OF SAMPLE NO. S/N 091-432 at 300 X
AFTER MAJOR DEFORMATION

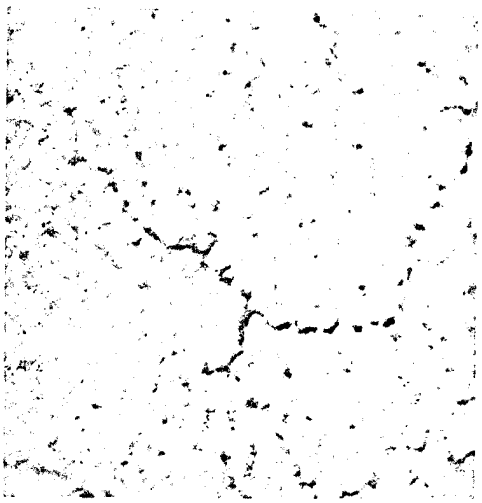

FIGURE 14
OPTICAL PHOTOMICROGRAPH
OF SAMPLE NO. S/N 091-426 AT 110X
SHOWING CRACKS BEFORE DEFORMATION

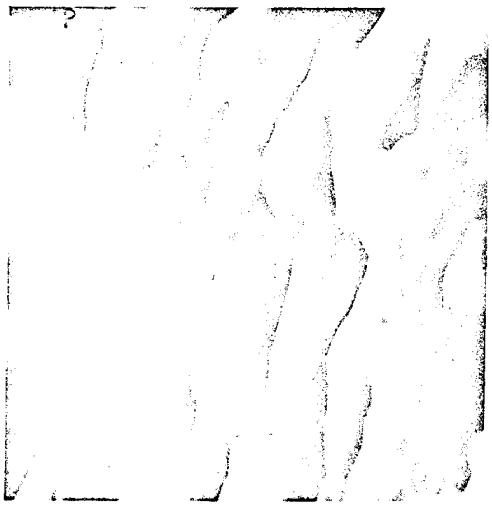

FIGURE 13
SCANNING ELECTRON PHOTOMICROGRAPH
OF SAMPLE NO. S/N 091-432 AT 5,000X
AFTER MAJOR DEFORMATION

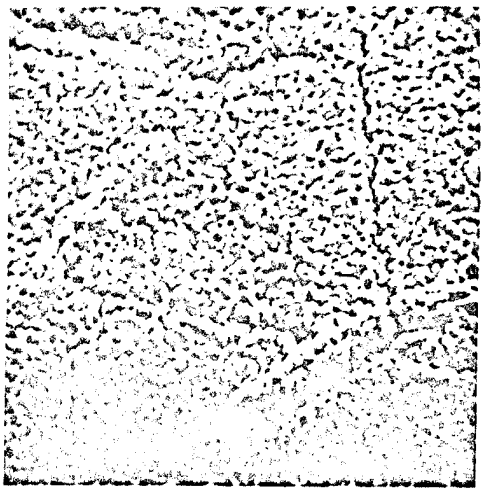

FIGURE 15
SCANNING ELECTRON PHOTOMICROGRAPH
OF SAMPLE NO. S/N 091-426 AT 300X
SHOWING CRACKS BEFORE DEFORMATION